RSC Advances

ROYAL SOCIETY OF CHEMISTRY

www.rsc.org/advances

Poly (3,4-ethylenedioxythiophene): polystyrene sulfonate zirconium(IV) phosphate (PEDOT:PSS-ZrP) compsite ionomeric membrane for artifical muscle applications

Inamuddin[a], R.K. Jain[b], Sardar Hussain[a], Mu. Naushad[c]

[a] Department of Applied Chemistry, Faculty of Engineering and Technology, Aligarh Muslim University (AMU), Aligarh, 202002, India

[b] CSIR-Central Mechanical Engineering Research Institute, (CSIR-CMERI), Durgapur, 713209, West Bengal, India

[c] Department of Chemistry, College of Science, Building # 5, King Saud University, Riyadh, Saudi Arabia

Abstract

The PEDOT:PSS-ZrP ionomeric actuator was developed for artificial muscle applications. The polyvinyl chloride (PVC) based (PEDOT:PSS) Zr(IV) phosphate composite ionomeric membrane (PVC-PEDOT:PSS-ZrP) was successfully synthesized by solution casting technique. Various instrumental techniques including thermogravimetric analysis/differential thermal analysis/differential thermogravimetry (TGA/DTA/DTG), energy dispersive X-ray (EDX) analysis, scanning electron microscopy (SEM), X-ray diffraction (XRD) and Fourier transform infrared (FT-IR) spectroscopy were used to characterize the PVC-PEDOT:PSS-ZrP ionomeric material. Membrane properties were evaluated in terms of ion exchange capacity, cyclic and linear sweep voltammetry, water uptake, water loss and proton conductivity. The tip displacement of PVC-PEDOT:PSS-ZrP composite ionomeric membrane was also studied. The composite ionomeric membrane showed excellent displacement under applied voltage. Therefore, composite ionomeric membrane was found suitable for bending actuation applications in artificial muscles.

Keywords; PVC-PEDOT:PSS-ZrP ionomeric membrane, ion exchange capacity, tip displacement, artificial muscle application.

Author information

E-mail: inamuddin@rediffmail.com

1. Introduction

In recent years ionic polymer metal composites (IPMCs) have established themselves as most appropriate material for artificial muscle, bio-mimetic, robotics and sensors applications due to their lighter weight, flexibility, precise sensing ability etc. **[1-15].** An IPMC is basically made by coating of both the sides of ionomeric membrane with noble metal. Oguro and Asaka first developed IPMC actuator using nafion membrane surface coated with gold or platinum **[16,17]**. At an optimum applied voltage IPMC actuator bends from cathode to anode side due to the movement of cations along with water molecules. This phenomenon of bending of an IPMC membrane is known as actuation. An IPMC with good ion-exchange capacity (IEC) and proton conductivity (PC) is capable to offer large actuation under low applied voltage **[18-20]**. But IPMCs have some serious drawbacks including high cost, hysteresis, deformation at higher temperature, high evaporation rate of water molecules under applied voltage, time consuming electroless plating of metal, humidity, leakage from damage, porous surface and electrolysis etc. **[21-24]**. These factors degenerate the performance of actuator and gradually decrease the accuracy of measurement. Hence, alternate materials for IPMCs are always needed. For this purpose, hybrid ionomeric membranes obtained by embedding conducting polymer based ion exchangers as electroactive material in a polymer binder, *i.e.* PVC, are proposed to be viable alternative to the time consuming and costly method of electroless plating. These types of membranes may exhibit several outstanding properties as a result of combination of properties of inorganic exchangers and organic polymers such as excellent ion exchange capacity, mechanical stability, flexibility and water retention capacity **[25-27]**. The conducting polymers may have various advantages such as easy processability, cost effectiveness and good electrical conductivity and may have numerous important applications in nanoactuators and artificial muscles **[28-30]**. In recent years, poly(3,4 ethylenedioxythiophene): polystyrene sulfonate

(PEDOT:PSS) has emerged as excellent material for actuation as its offers several outstanding properties such as easy synthesis, cost effectiveness, electrochemical redox properties and most importantly high conductivity **[31-34]**. In the present research work, PVC-PEDOT:PSS-ZrP composite ionomeric membrane was utilized for the development of actuator applicable for artificial muscle applications. In this ionomeric membrane PVC binds with composite ion exchange material PEDOT:PSS-ZrP and provides mechanical stability to ionomeric membrane whereas conducting polymer PEDOT:PSS provides the redox cyclability under applied voltage. Various physico-chemical properties of ionomeric membrane were studied by various instrumental techniques such as XRD, FT-IR, SEM, EDX and TGA/DTA/DTG. Some of the ionomeric membrane electrochemical characterizations are also carried out to understand the bending actuation performance.

2. Materials and methods

2.1 Materials

The main reagents used for synthesis of ion exchange membranes were zirconium oxychloride octahydrate ($ZrOCl_2.8H_2O$) and dioctyl phthalate (Central Drug House, India), ortho-phosphoric acid (H_3PO_4), tetrahydro furan (THF) and liquor ammonia solution (Fischer Scientific, India), poly(3,4-ethylenedioxythiophene): polystyrene sulfonate (PEDOT:PSS), 1.3 wt% dispersion in H_2O, (Sigma Aldrich, India) and polyvinyl chloride (Otto Chemicals, India).

2.2. Instruments

A FT-IR spectrometer (Interspec-20, Spectrolab, U.K.), X-ray diffractometer (Miniflex-II, Japan), TGA/DTA analyzer (EXSTAR, TG/DTA-6300), scanning electron microscope (JEOL, JSM-6510 LV, Japan), an Autolab 302N modular potentiostat/galvanostat with impedance analyzer (FRA32M.X) (Switzerland), laser displacement sensor (OADM 20S4460/S14F, Baumer Electronic, Germany), load cell (Citizen CX-220, India), pH meter, oven, balance and magnetic stirrer (Elico LI-120, Jindal Scientific Instrumentation, Wensar, MAB-220 and Labman LMMS-1L4P, India, respectively) were used.

2.3. Synthesis of composite ionomer

Composite ionomer PEDOT:PSS-ZrP was synthesized according to the method reported by Mohammad et al. **[35]**. It was prepared by mixing 0.4 M $ZrOCl_2.8H_2O$ and 2.25 M H_3PO_4 solutions in 1:3 volume ratios at a pH of 1 and finally 2 mL of PEDOT:PSS was added. The synthesized hybrid material was digested at room temperature for about 24h, decanted, washed and dried at 45°C ± 0.5°C. The IEC was calculated as per the reported method **[35]**.

2.4. Membrane Preparation

Coetzee and Benson [36] method was followed for the preparation of the ionomeric membrane of PEDOT:PSS-ZrP. The PEDOT:PSS-ZrP ionomeric material was grinded to fine powder. A 1 g portion of PEDOT:PSS-ZrP powder was added into the gel of 0.2g PVC powder prepared in 10 ml of THF followed by adding of 50 µL of dioctylphthalate plasticizer [37]. It was mixed thoroughly with the help of magnetic stirrer. The solution was transferred into a Petri dish (diameter 10 mm). The thin PVC-PEDOT:PSS-ZrP membrane was obtained after slow evaporation of THF.

2.5. Ion exchange capacity (IEC)

The IEC of composite ionomeric membrane was determined by standard column process as discussed elsewhere [35]. The IEC was calculated with the help of Eq. (1):

$$\text{IEC} = \frac{V \times N}{W} (\text{meq g}^{-1} \text{ dry membrane}) \ldots\ldots\ldots (1)$$

where, V and N are the volume and normality of NaOH consumed, W is the weight of ionomeric membrane.

2.6. Proton conductivity (PC)

The PC of PVC-PEDOT:PSS-ZrP composite ionomeric membrane (30×10×0.15 mm) (length × width × thickness) was measured by an impedance analyzer. Before performing the experiment, the IMPC membrane was soaked in demineralised water for 12 h. The PC of IPMC membrane was measured in water at room temperature (25 ± 2°C). The PC (σ) was calculated by applying Eq. (2):

$$\sigma = \frac{L}{R \times A} \ldots\ldots\ldots\ldots\ldots (2)$$

where, σ, L, A, R are PC (S cm^{-1}), thickness of membrane (cm), cross-sectional area of membrane (cm^2) and the resistance (Ohm), respectively.

2.7. Water uptake

The pre-weighed PVC-PEDOT:PSS-ZrP composite dry ionomeric membrane was kept in demineralised water. The effect of time and temperature for the water uptake was studied at room temperature (25 ± 2°C) and 45°C for different time intervals. The water uptake was calculated by using Eq. (3) as follows:

$$\text{Water uptake (\%)} = \frac{W_w - W_d}{W_w} \quad \text{.....(3)}$$

where, W_w and W_d are the weights of the soaked/wet and dry membranes, respectively.

2.8. Water loss

The PVC-PEDOT:PSS-ZrP composite ionomeric membrane was soaked in demineralised water for 24 h. After soaking membrane was wiped with Whatman's filter paper and weighed. Pre-weighed membrane was subjected to constant electric voltage of 3V for different time span ranging from 3-12 min. After applying the voltage the membrane was weighed again and %water loss was calculated by using Eq. (4) :

$$\text{Water loss (\%)} = \frac{W_b - W_a}{W_b} \quad \text{.....(4)}$$

where, W_w and W_d are the weights of the soaked/wet and dry membranes observed before and after applying the voltage, respectively.

2.9. Electromechanical study

The cyclic voltammetry study of PVC-PEDOT:PSS-ZrP composite ionomeric membrane was studied in the potential range of -8 to 8 V. The linear sweep voltammetry study of PVC-PEDOT:PSS-ZrP composite ionomeric membrane was studied by applying the voltage of 0-7 V.

2.10. Instrumental analysis

SEM images of PVC-PEDOT:PSS-ZrP composite ionomeric membranes were captured by scanning electron microscope at an accelerating voltage of 20 kV. A typical Energy dispersive X-ray spectrum was reordered during SEM analysis. X-ray diffraction pattern of PVC-PEDOT:PSS-ZrP composite ionomeric membrane was recorded by using X-Ray diffractometer with Cu Kα radiation. The FT-IR spectrum of PVC-PEDOT:PSS-ZrP composite ionomeric membrane was recorded in the range of 4000-400 cm^{-1} by using FT-IR spectrometer. The TGA/DTA/DTG analysis of PVC-PEDOT:PSS-ZrP composite ionomeric membrane under nitrogen atmosphere with heating rate of 20 ^{o}C min^{-1} from 25-1450^{o}C was investigated by using thermogravimetric analyser.

3. Results and discussion

The PVC-PEDOT:PSS-ZrP composite ionomeric membrane prepared by solution casting method possessed significant IEC of 1.10 meq g^{-1} of dry membrane and also exhibited excellent PC of 2.42 × 10^{-6} Scm^{-1} **(Table 1)**. The good IEC and PC of PVC-PEDOT:PSS-ZrP composite ionomeric membrane may be accountable for higher water uptake **[38]**. The presence of reasonable water on the membrane may result in quick movement of more hydrated cations towards cathode thereby creating an appropriate pressure on anode, resulting in larger and faster actuation **(Fig. 1)**. The higher water uptake property of the ionomeric membrane is accountable for the enhanced performance of actuator. The water uptake capacity of PVC-PEDOT:PSS-ZrP composite ionomeric membrane at room temperature (25 ± 2°C) increases with the increase of immersion time up to 16 h and after that saturation was established (**Fig. 2)**. The percentage of water uptake at room temperature (25±2°C) with immersion time 16h was found 9.52%. The percentage of water uptake of composite ionomeric membrane at elevated temperature (45°C) was found to be 8.92%. The results showed that only 0.6% of water holding capacity of membrane was lost at 45°C. **(Fig. 2)**. The water retion capability even at elevated temperature may be due to the presence of more active thermally enlarged PO_4^{2-} groups on composite cation exchange membrane. The high water uptake of composite ionomeric membrane at elevated temperature may also facilitate the movement of hydrated cation even in case of high temperature leading to the good actuation. The water loss of pre-weighed PVC-PEDOT:PSS-ZrP composite ionomeric membrane was observed by applying an electric voltage of 3V at different interval of time, i.e., 3 , 6, 9 and 12 min. It was observed that the water loss of membrane was found to be dependent on time and loss increases with increase in time **[39]**. However, only 1.82% water loss was observed at an applied voltage of 7 V for 12 min **(Fig. 3)**. The loss of water may be due to the water leakage from damaged surface of membrane. The electrical property of

PVC-PEDOT:PSS-ZrP composite ionomeric membrane was explored by employing potentiostatic cyclic voltammetry. The quick movement of the hydrated ions because of the applied electrical voltage with decomposition profile of water due to electrolysis reflects the shape of I–V hysteresis curves. It was noted that the slope of I–V curve for composite ionomeric membrane is showing slight hysteresis in oxidation and reduction current **(Fig. 4)**. The current density of composite ionomeric membrane was obtained by applying voltage of 7V and found that it increases with increase in voltage as shown in **Fig. 5**. The elemental composition of PVC-PEDOT:PSS-ZrP composite ionomeric membrane is presented in **Table 2**. The results showed the presence of elements such as C, O, Zr, P and Cl which confirms the formation of PVC-PEDOT:PSS-ZrP composite ionomeric membrane **(Fig. 6).** The XRd pattern of PVC-PEDOT:PSS-ZrP composite ionomeric membrane showed very small peaks of 2θ values suggesting the amorphous nature of hybrid cation exchange membrane **(Fig. 7)**. The FT-IR spectrum of PVC-PEDOT:PSS-ZrP composite ionomeric membrane **(Fig. 8)** shows the presence of –OH stretching of external water molecule (3436 cm^{-1}) **[40]**, metal oxygen bond (Zr-O) (608 cm^{-1}) **[41]**, ionic phosphate (517, 1074 cm^{-1}) **[42]**, C=O stretching (1734 cm^{-1}) **[43]**, lattice (internal) water (1636 cm^{-1}) **[44]** and C-H stretching mode for polyvinyl chloride (2926 cm^{-1}) **[45]**. The thermogram of PVC-PEDOT:PSS-ZrP composite ionomeric membrane **(Fig. 9)** exhibited good thermal stability as it retained 50% of mass by heating upto 600 ^{o}C. When hybrid cation exchange membrane was heated upto 100^{o}C only 6.12% loss in weight was resulted which may be due to the removal of external water molecules attached to the surface of composite ionomeric membrane. On further heating upto 200^{o}C, 10.06% weight loss is noticed which is accounted for the removal of water molecules which were strongly coordinated in composite ionomeric membrane **[46]**. Another mass loss of 18.7% was observed while heating the material upto 248^{o}C whereas further increase in temperature upto 336^{o}C showed 8% weight loss which is considered due to PEDOT:PSS

decomposition [47]. Conversion of phosphate group into pyrophosphate was considered with 1.6% weight loss upto 401^{o}C [48]. Further, 5.17% weight loss was observed by heating upto 600^{o}C which was associated with decomposition of organic polymer polyvinyl chloride [49]. The DTA curve showed two sharp peaks at 336 and 550^{o}C which are confirming the transition associated in TGA analysis. Beyond 600^{o}C, almost horizontal curve represented the formation of oxides [50]. SEM images of the PVC-PEDOT:PSS-ZrP composite ionomeric membrane before and after applying electrical voltage of 7V are shown in **Fig. 10 (a-b)**. Fresh hybrid membrane showed smooth surface morphology without any type of spaces whereas after applying voltage surface morphology of hybrid membrane becomes slightly rough without development of any visible rapture. Thus, it was observed that after applying the voltage hybrid membrane was overall not much affected. SEM microphotographs presented in **Fig. 10 (c-d)** shows the cross-sectional images of PVC-PEDOT:PSS-ZrP composite ionomeric membrane. Which indicated that the PEDOT:PSS-ZrP composite ion exchanger particles are deeply embedded in the in the matrix of polyvinyl chloride. The denser aggregation of cation exchanger particles in composite ionomer results compact granular filling which is responsible for lesser degree of water loss from hybrid cation exchanger membrane.

After attempting the micro-structure property, we are focused on the electromechanical properties of PVC-PEDOT:PSS-ZrP composite ionomeric actuator where the bending capabilities of this actuator are analyzed. For analyzing these properties, an experimental testing setup is designed as shown in Fig .11. The ionomeric actuator is mounted in a fixture. For applying the voltage (0-7.0 VDC), a customized control system is developed where this control system consists of digital analog card (DAC), micro controller with PD control system and an amplifier circuit along with power supply. A laser displacement sensor is utilized to measure the tip displacement of ionomeric actuator. The main function of this laser

displacement sensor is to provide the feedback during sending the controlled voltage to the actuator so that accurate bending can be achieved. In order to find the electro mechanical properties of the membrane, the schematic diagram of experimental testing setup is shown in **Fig. 11**. When voltage (0-7 V) is applied to the membrane through a customized control system, the tip displacement is controlled through PC interface as an input command. The data from RS-485 to RS-232 protocol is converted by a convertor. The data is collected by Docklight V1.8 software through RS-232 port in a computer. Using C programming language, a computer code is written where the sampling rate (20 samples per second) is given in the software for controlling the membrane. The actuator bends at voltage (0-7 VDC) as shown in **Fig. 12.** During experimentation, the size of actuator (30×10×0.15 mm) (length × width × thickness) is taken and the deflection pictures are captured at different voltages (0-7.0 DC) as shown in **Fig. 13.** By conducting repeated tests, the deflections are collected at different voltages as shown in **Table 3**. The averages of five values at corresponding voltages are plotted in **Fig. 14**. It is found that the maximum deflection is 15 mm at 7.0 V and also shows the steady state behaviour. It is also observed that when the voltage reduces from 7.0 to 0 V, PVC-PEDOT:PSS-ZrP composite ionomeric membrane does not attempt in the similar behaviour and it shows error in deflection (0.5 mm). This can be minimized using a PD control system. In the PD control system, PD gains are tuned by setting a frequency in the controller and error is minimized.

In order to observe the force behavior of PVC-PEDOT:PSS-ZrP composite ionomeric actuator, this is clamped in a cantilever mode a holder as shown in **Fig. 15** . A load force cell is located under the tip of ionomeric actuator for finding the tip load. The low force measurement load cell is used which can compute the load ranging between 0.0001- 220g. Before actuation of IPMC, the load cell is tarred with the weight of IPMC. When voltage (0-7 V) is applied to this ionomeric actuator, the tip of this IPMC moves upward and downward according to the polarity of voltage. The weight of water left is neglected and the different

five load values are noted by the load cell at respective voltage. These are denoted by F_1, F_2, F_3, F_4 and F_5 as given in **Table 4.** The calculated standard deviation (SD) and means values are 0.6983 and 0.795, respectively. The normal distribution function (NDF) for PVC-PEDOT:PSS-ZrP composite ionomeric actuator is shown in **Fig. 16**. By using normal distribution function, the repeatability of PVC-PEDOT:PSS-ZrP composite ionomeric actuator is calculated as 99.70% which can be used for artificial muscle application.

4. Conclusion

In this study, PVC-PEDOT:PSS-ZrP composite ionomeric membrane was prepared by solution casting method to explore actuation performance. The good IEC and PC are accounted for the faster actuation of hybrid cation exchange membrane. The composite ionomeric membrane was also having excellent water uptake capacity and lesser amount of water loss. The tip displacement parameters revealed fast actuation of composite ionomeric membrane. Thus, PVC-PEDOT:PSS-ZrP composite ionomeric membrane could be effectively utilized in artificial muscle application which will open new window of opportunities in the area of artificial muscles.

Acknowledgements

The authors are thankful to Department of Applied Chemistry, Aligarh Muslim University, India for providing research facilities and the Department of Science and Technology for the Young Scientist award to Dr. Inamuddin, Project No. SR/FT/CS-159/2011. The authors are also thankful to CSIR-CMERI, Durgapur, India for carrying out of the electromechanical characterization and demonstration of IPMC based microrobotic system at DMS/Micro Robotics Laboratory, CSIR-CMERI, Durgapur, India. One of the authors (Mu. Naushad) acknowledges the King Saud University, Deanship of Scientific Research, College of Science Research Center for the support.

5. References

1. R. Dong and Y. Tan, *Sensor and Actuator A: Physical,* 2015, **224**, 43.
2. M. Shahinpoor and K. J. Kim, *Smart Mater. Struct.,* 2001, **10**, 819.
3. K. J. Kim and M. Shahinpoor, *Smart Mater. Struct.*, 2003, **12,** 65.
4. Y. Cha, H. Kim and M. Porfiri, *Material Letter,* 2014, **133**, 179.
5. C. Jo, D. Pugal, I.K. Oh, K.J. Kim and K. Asaka, *Progress in Polymer Science*, 2013, **38**, 1037.
6. M. Annabestani and N. Naghavi, *Sensor and Actuators A: Physical*, 2014, **209**, 140.
7. Y. Tang, Z. Xue, X. Zhou, X. Xie and C.Y. Tang, *Sensors and Actuators B: Chemical*, 2014, **202**, 1164.
8. R. K. Jain, S. Datta and S. Majumder, *Mechatronics*, 2013, **23**, 381.
9. R. K. Jain, S Datta and S. Majumder, *Mechanics Based Design of Structures and Machines: An International Journal*, 2014, **42**, 398.
10. R. K. Jain, S. Majumder and A. Dutta, *Robotics and Autonomous Systems*, 2013, **61**, 297.
11. S. Tung, S. R. Witherspoon, L. A. Roe, A. Silano, D. P. Maynard and N. Ferraro, *Smart Materials & Structures*, 1999, **10**, 1230–9.
12. S. W. Yeom and I. K. Oh, *Smart Materials & Structures,* 2009, **18**, 085002.
13. R. Lumia and M. Shahinpoor , *Journal of Physics*, 2008, **127**, 1−15.
14. Y. Bar-Cohen and Q. M. Zhang, *MRS Bull,* 2008, **33**, 173−181.
15. Oguro K, Asaka K and Takenaka H 1993 Actuator element US Patent Specification 5, 268, 08.
16. Z. Y. Cheng, T. B. Xu, V. Bharti, S. X. Wang and Q. M. Zhang, *Applied Physics Letters,* 1999, **74**, 1901−1903.

17. H. Okuzaki, S. Takagi, F. Hishiki and R. Tanigawa, *Sensors and Actuators B: Chemical*, 2014, **194**, 59.

18. B.K. Fang, C.C.K. Lin and M.S. Ju, *Sensors and Actuators A: Physical*, 2010, **158**, 1.

19. Inamuddin, A. Khan, R. K. Jain and M. Naushad, *Smart Materials & Structures,* 2015, **24**, 095003 (14pp).

20. Inamuddin, A. Khan, R. K. Jain and M. Naushad, *Journal of Intelligent Material Systems and Structures*, 2015, doi: 1045389X15596627.

21. P. Brunetto, L. Fortuna, P. Giannone, S. Graziani and S. Strazzeri, *IEEE Transactions on Instrumentation and Measurements*, 2010, **59**, 893.

22. X. Zhao and Y. Tan, *Sensor and Actuators A: Physical*, 2006, **126**, 306.

23. Inamuddin, A. Khan, M. Luqman and A. Dutta, *Sensors and Actuators A: Physical*, 2014, **216**, 295.

24. M.M.A. Khan, Rafiuddin and Inamuddin, *Journal of Environmental Chemical Engineering*, 2014, **2**, 471.

25. M.M.A. Khan, Rafiuddin and Inamuddin, *Material Science and Engineering: C*, 2013, **33** 2360.

26. A.A. Khan, A. Khan and Inamuddin, *Talanta*, 2007, **72**, 699.

27. Z. Alam, Inamuddin and S.A. Nabi, *Desalination*, 2010, **250**, 515.

28. T. Tevi, S.W.S. Birch, S.W. Thomas and A. Takshi, *Synthetic Metals*, 2014, **191**, 59.

29. M. Shahinpoor, Y. Bar-Cohen, J. O. Simpson and J. Smith, *Smart Materials & Structures,* 1998, **7**, R15.

30. S. Nemat-Nasser and J. Y. Li, *Journal of Applied Physics,* 2000, **87**, 3321.

31. F. Zabihi, Y. Xie, S. Gao and M. Eslamian, *Applied Surface Science*, 2015, **338**, 163.

32. S. van Reenen, M. Scheepers, K. van de Ruit, D. Bollen and M. Kemerink, *Organic Electronic*, 2014, **15**, 3710.

33. C.O. Baker, B. Shedd, P.C. Innis, P.G. Whitten, G.M. Spinks, G.G.Wallace and R.B. Kaner, *Advance Materials*, 2008, **20**, 155.

34. J. Huang, P.F. Miller, J.C. de Mello, A.J. de Mello and D.D.C. Bradley, *Synthetic Metals*, 2003, **139**, 569.

35. A. Mohammad, Inamuddin and S. Hussain, Ionics, 2015, **21**, 1063.

36. C.J. Coetzee and A.J. Benson, *Analytica Chimca Acta*, 1971, **57**, 478.

37. A. Craggs, G.J. Moody and J.D.R. Thomas, Journal Chemical Education, 1974, **51**, 541.

38. V. K. Nguyen, J. W. Lee and Y. T. Yoo, *Sens. Actuator B Chem.*, 2007, **120,** 529.

39. M. Shahinpoor, *Electrochim. Acta*, 1999, **48**, 2343.

40. A. Hebeish, A. Higazy, A. El-Shafei and S. Sharaf, *Carbohydrate. Polymer*, 2010, **79**, 60.

41. K.G. Varshney, V. Jain and N. Tayal, *Indian Journal of Chemical Technology*, 2003, **10**, 186.

42. C. Ruan, F. Yang, J. Xu, C. Lei and J. Deng, *Electroanalysis*, 2005, **9**, 1080.

43. K.G. Varshney, A. Agrawal and S.C. Mojundar, *Journal of Thermal Analytical Calorim*etry, 2005, **81**, 183.

44. A. Nilchi, B. Maalek, A. Kanchi, M.G. Maragheh and A. Bagheri, *Radiation Phyics and Chemistry*, 2006, **75**, 301.

45. S. Ramesh, K.H. Leen, K. Kumutha and A.K. Arof, *Spectrochimica Acta Part A*, 2007, **66**, 1237.

46. C. Duval, Inorganic Thermogravimetric Analysis, Elsevier, Amsterdam (1953), p. 403.

47. S. Letaief, P. Aranda, R. Fernandez-Saavedra, C. James, J. Margeson, C. Detellier and E. Ruiz-Hitzky, *Journal of Material Chem*istry, 2008, **18**, 2227.

48. A. Lagashetty, V. Havanoor, S. Basavaraja and A. Venkataraman, *Bulletin of Material Science*, 2005, **28**, 477.

49. A.S. Mahalle and V.S. Sangawar, Ionic conductivity of PVC based microporous polymer membrane electrolyte, *Chemical Science Transactions*, 2013, **2**, 322.

50. C. Duval, Inoganic Thermogravimetric Analysis, Elsevier, Amsterdam (1953) 492-497.

Caption of tables

Table 1

IEC and PC of PVC-PEDOT:PSS-ZrP membrane

Table 2

Elemental composition of PVC-PEDOT:PSS-ZrP membrane

Table 3

Deflection data with applied voltages for PVC-PEDOT:PSS-ZrP membrane

Table 4.

Force data of PVC-PEDOT:PSS-ZrP actuator

Caption of figures

Fig. 1. Graphical representation of bending mechanism for PVC-PEDOT:PSS-ZrP actuator.

Fig. 2. Water uptake of PVC-PEDOT:PSS-ZrP actuator.

Fig.3. Water loss after applying the voltage on PVC-PEDOT:PSS-ZrP membrane.

Fig. 4. Cyclic voltammetry curve for PVC-PEDOT:PSS-ZrP actuator.

Fig. 5. LSC curve for for PVC-PEDOT:PSS-ZrP actuator.

Fig. 6. EDX spectrum of composite ionomeric membrane PVC-PEDOT:PSS-ZrP.

Fig. 7. XRD pattern of PVC-PEDOT:PSS-ZrP membrane.

Fig. 8. FTIR spectrum of PVC-PEDOT:PSS-ZrP membrane.

Fig. 9. Simultaneous TGA/DTA/DTG curves of PVC-PEDOT:PSS-ZrP actuator.

Fig.10. SEM microphotographs of PVC-PEDOT:PSS-ZrP (a) before actuation (b) after actuation (c) cross-sectional images at magnification of 80× (d) cross-sectional images at magnification of 95×.

Fig. 11. Schematic diagram for bending response of PVC-PEDOT:PSS-ZrP actuator.

Fig. 12. Actual testing setup for bending response of PVC-PEDOT:PSS-ZrP actuator.

Fig. 13. Deflection response of PVC-PEDOT:PSS-ZrP membrane at different voltages.

Fig. 14. Bending response of PVC-PEDOT:PSS-ZrP actuator.

Fig. **15.** Force measurement testing setup for PVC-PEDOT:PSS-ZrP actuator**.**

Fig. 16. Normal distribution function (NDF) for PVC-PEDOT:PSS-ZrP actuator.

Table 1

Membrane composition						
PEDOT:PSS Zr(IV) phosphate (g)	**PVC (g)**	**Plasticizer (µL)**	**THF (mL)**	**Thickness (mm)**	**IEC (meq g^{-1} of dry membrane)**	**Proton conductivity (Scm^{-1})**
1	0.2	50	10	0.158	1.10	2.42×10^{-6}

Table 2

Elements	Weight%	Atomic%
C	59.96	73.84
O	21.91	20.25
Zr	7.48	1.21
Cl	6.46	2.70
P	4.19	2.00

Table 3

Voltage (V)	Deflection (Def.) values (mm)					Average deflection (mm)
	Def. 1	Def. 2	Def. 3	Def. 4	Def. 5	
0	0	0	0	0	0	0
1.0	0.9	1.0	0.8	1.1	1.2	1.0
2.0	3.5	3.6	3.4	3.5	3.5	3.5
3.0	5.1	4.9	5.0	5.2	4.8	5.0
4.0	7.6	7.5	7.4	7.5	7.5	7.5
5.0	9.4	9.5	9.6	9.6	9.4	9.5
6.0	10.9	11.1	10.8	11.2	11.0	11.0
7.0	15.0	15.2	14.9	14.8	15.1	15.0

Table 4

Voltage (V)	Force value (F_1) in mN	Force value (F_2) in mN	Force Value (F_3) in mN	Force Value (F_4) in mN	Force value (F_5) in mN	Average Force value (F) in mN
0	0	0	0	0	0	0
1.0	0.104	0.092	0.099	0.103	0.092	0.098
2.0	0.295	0.294	0.300	0.291	0.290	0.294
3.0	0.495	0.492	0.490	0.496	0.487	0.492
4.0	0.840	0.82	0.790	0.830	0.820	0.820
5.0	1.239	1.234	1.236	1.233	1.238	1.236
6.0	1.512	1.519	1.508	1.513	1.508	1.512
7.0	1.870	1.960	1.940	1.880	1.900	1.910

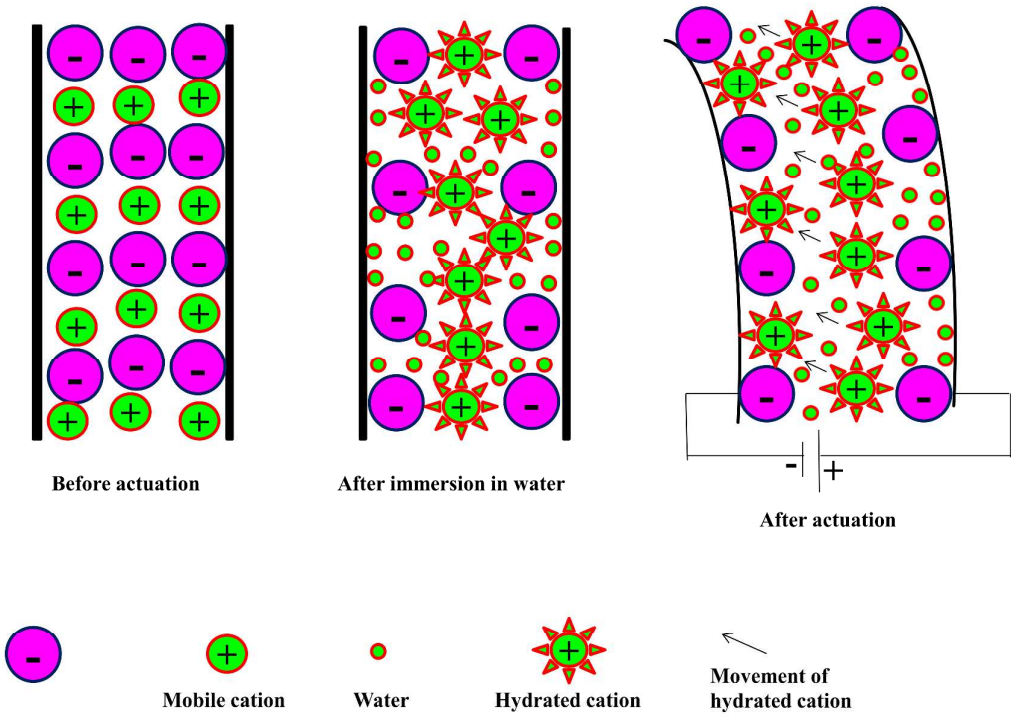

Fig. 1.

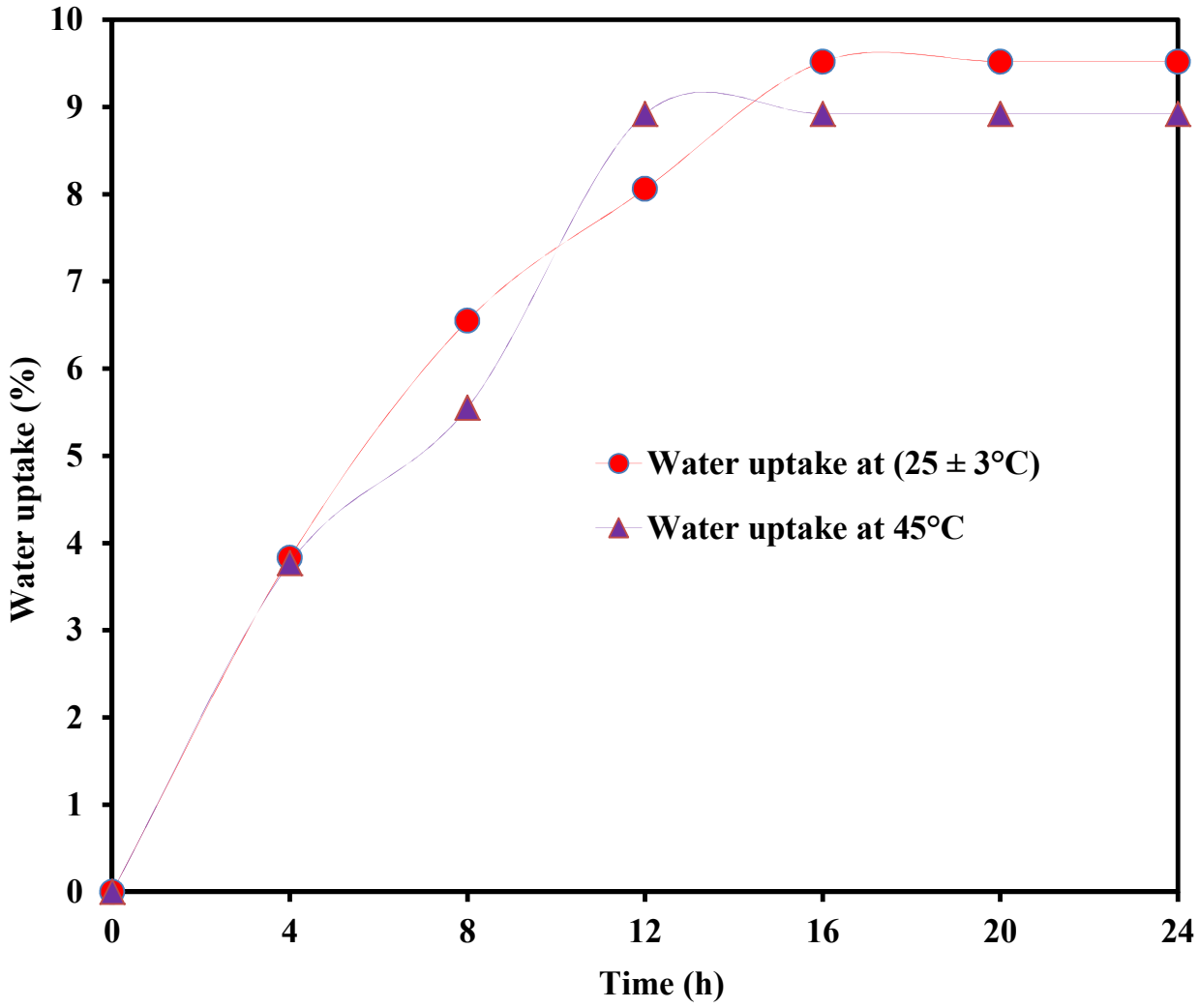

Fig. 2.

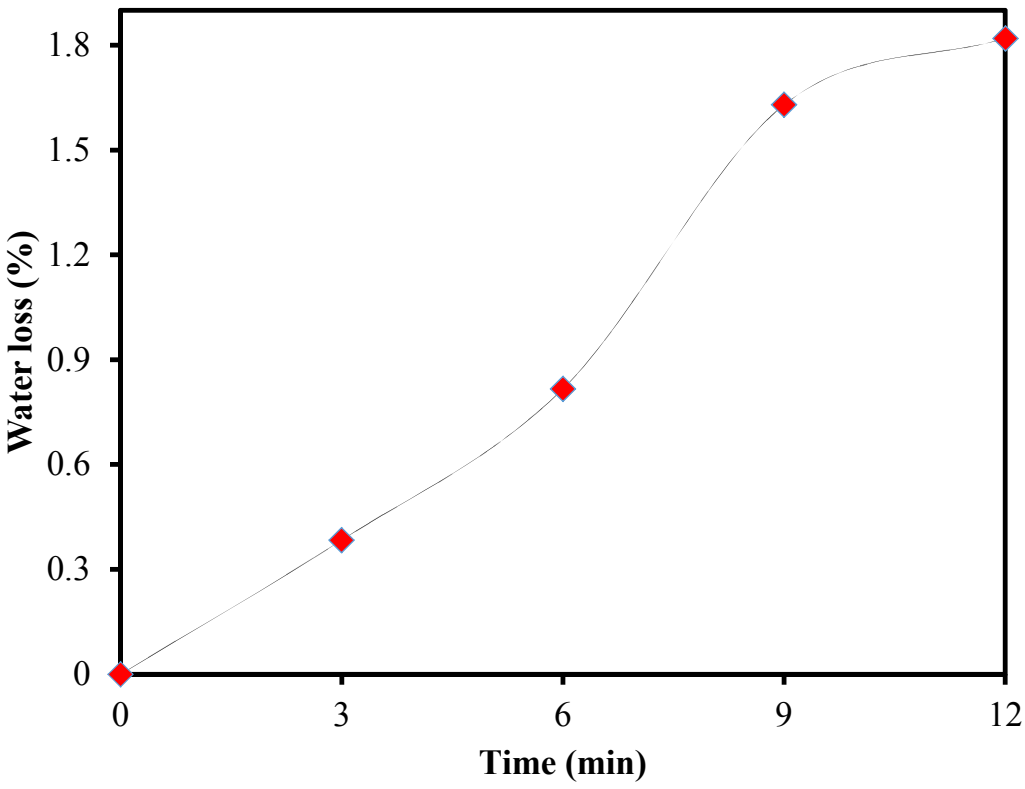

Fig. 3.

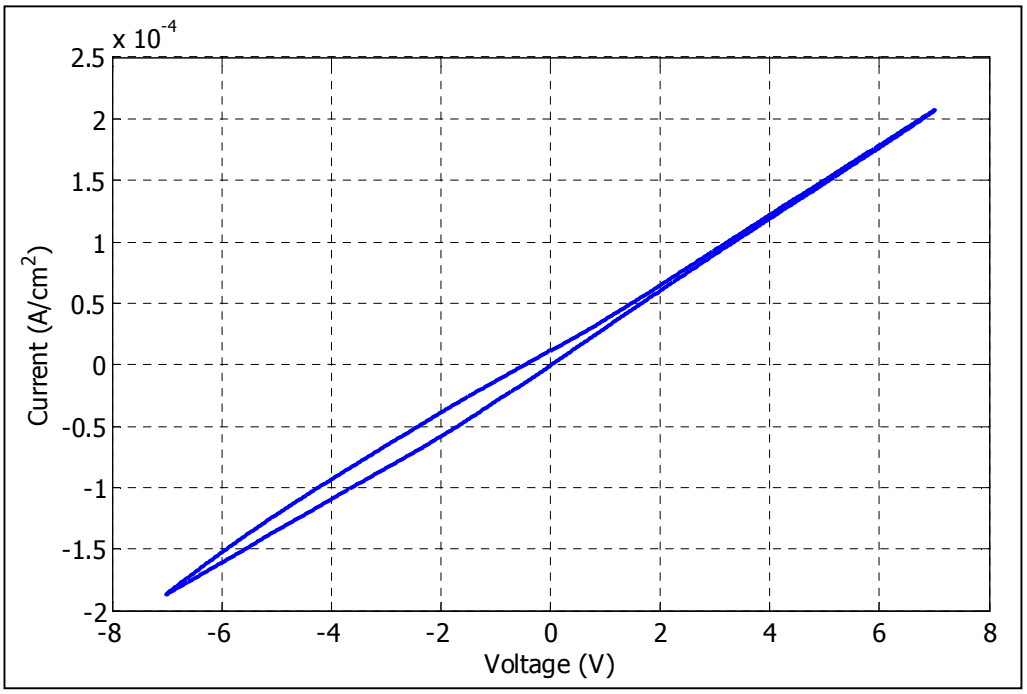

Fig. 4.

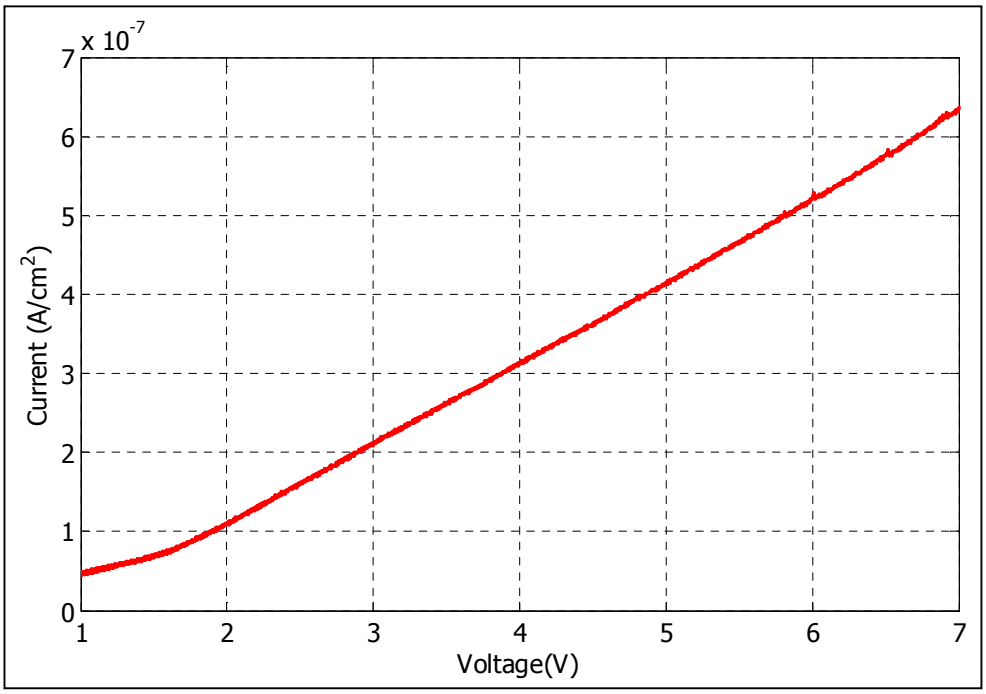

Fig. 5.

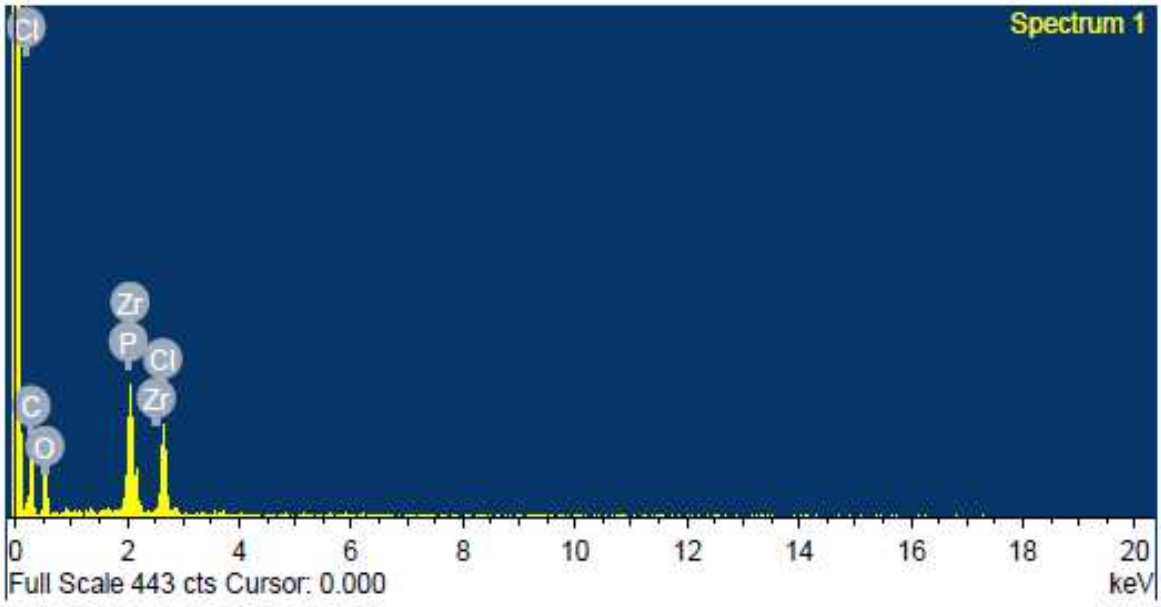

Fig. 6.

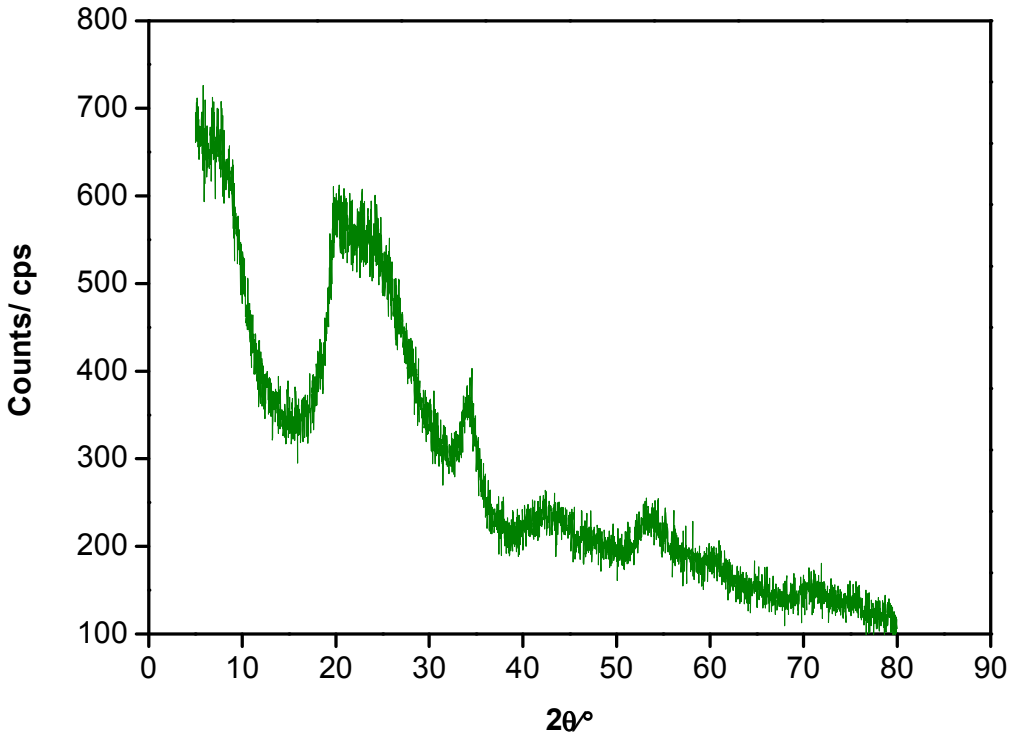

Fig. 7.

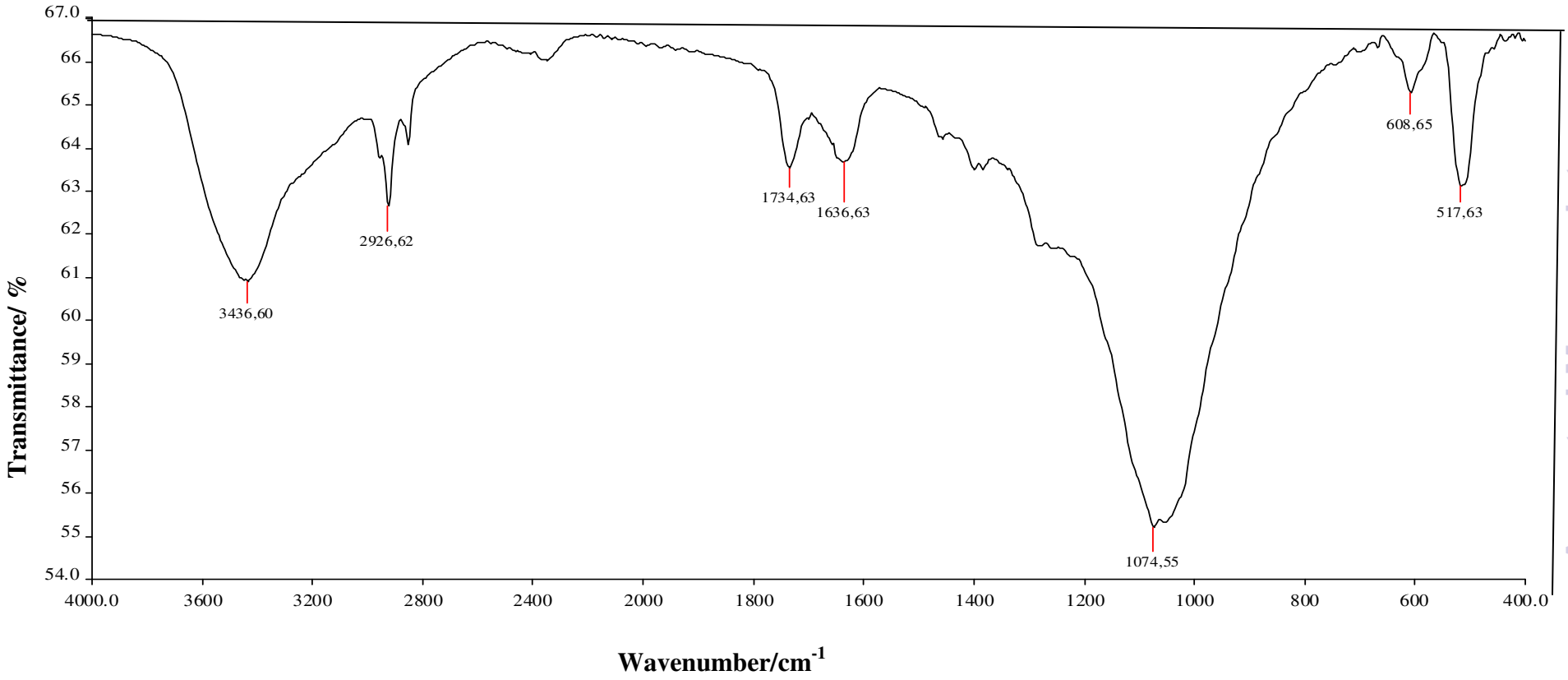

Fig. 8.

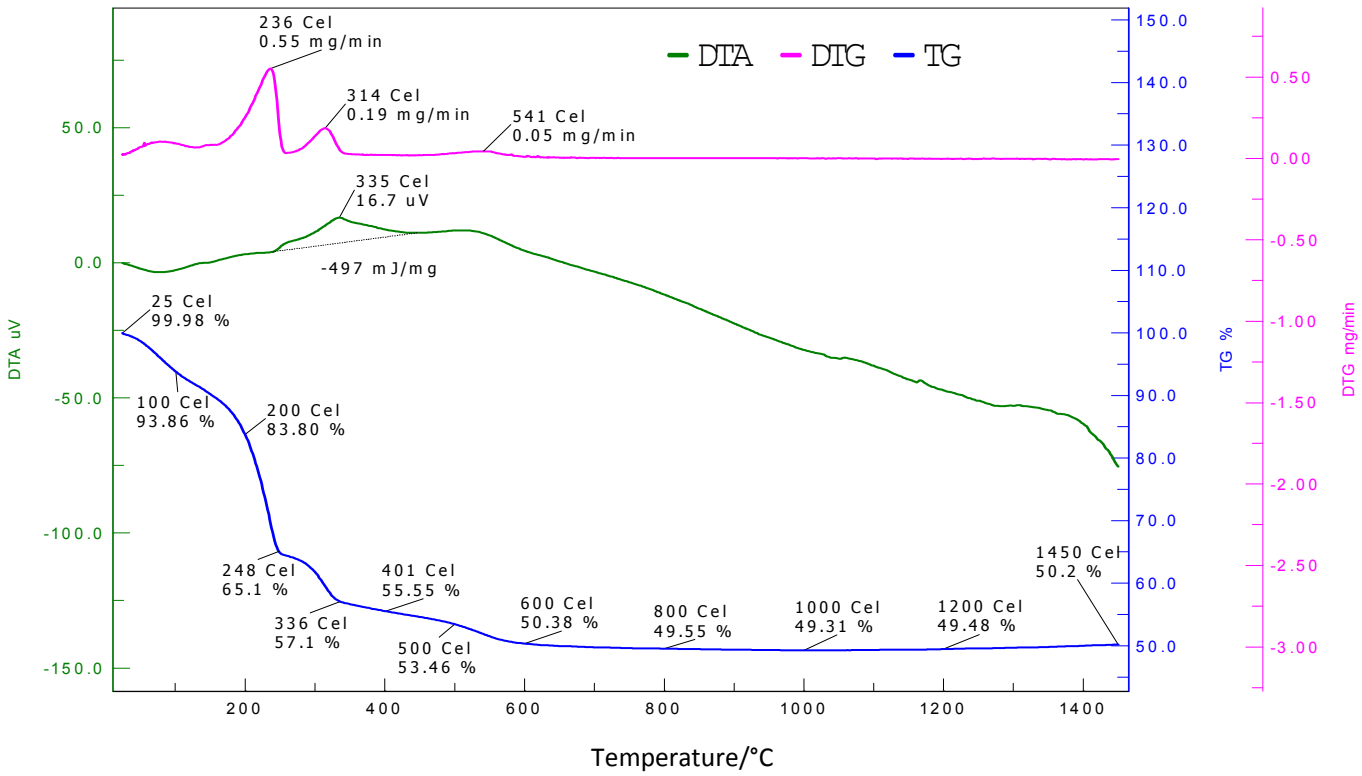

Fig. 9.

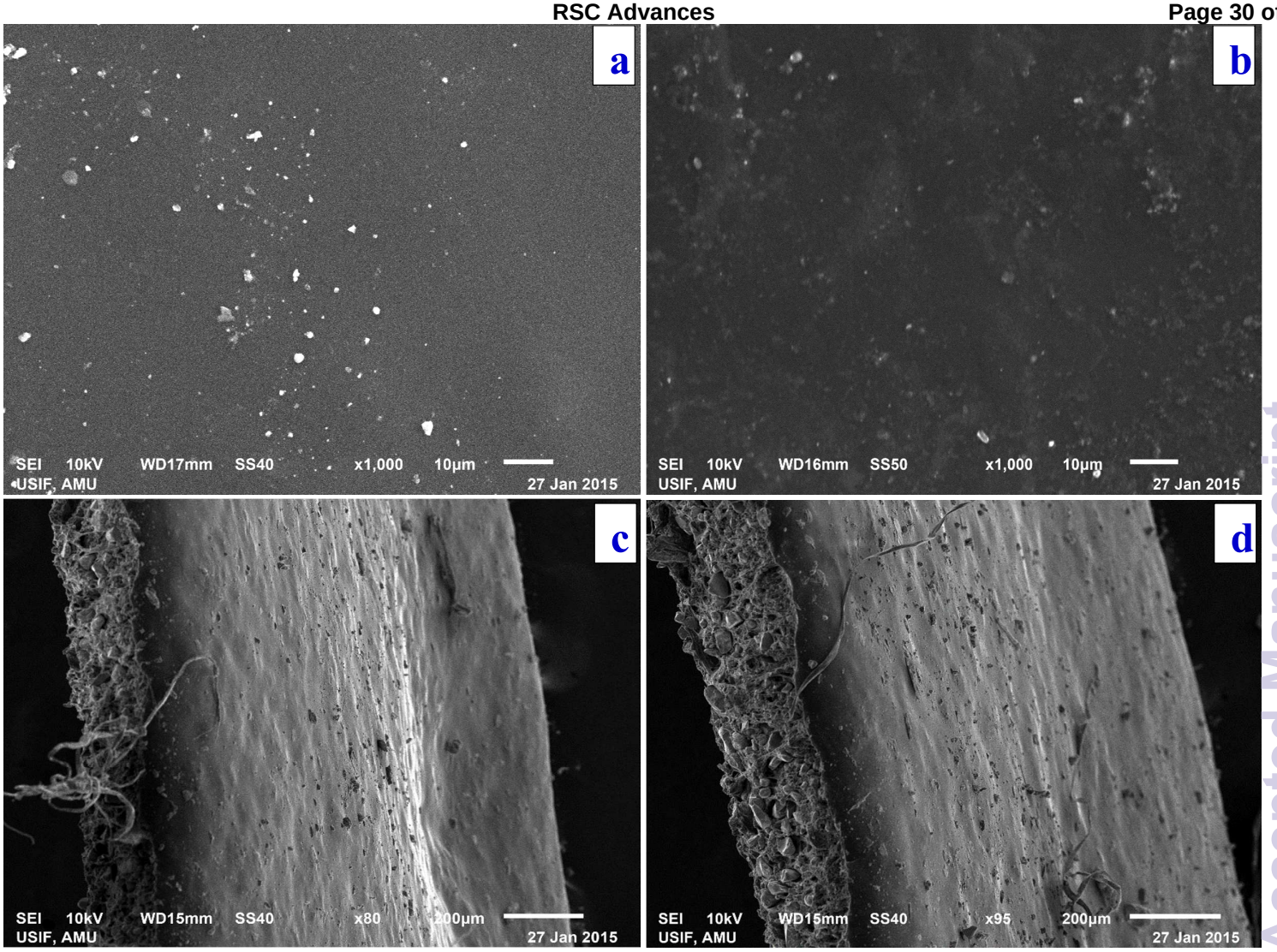

Fig. 10.

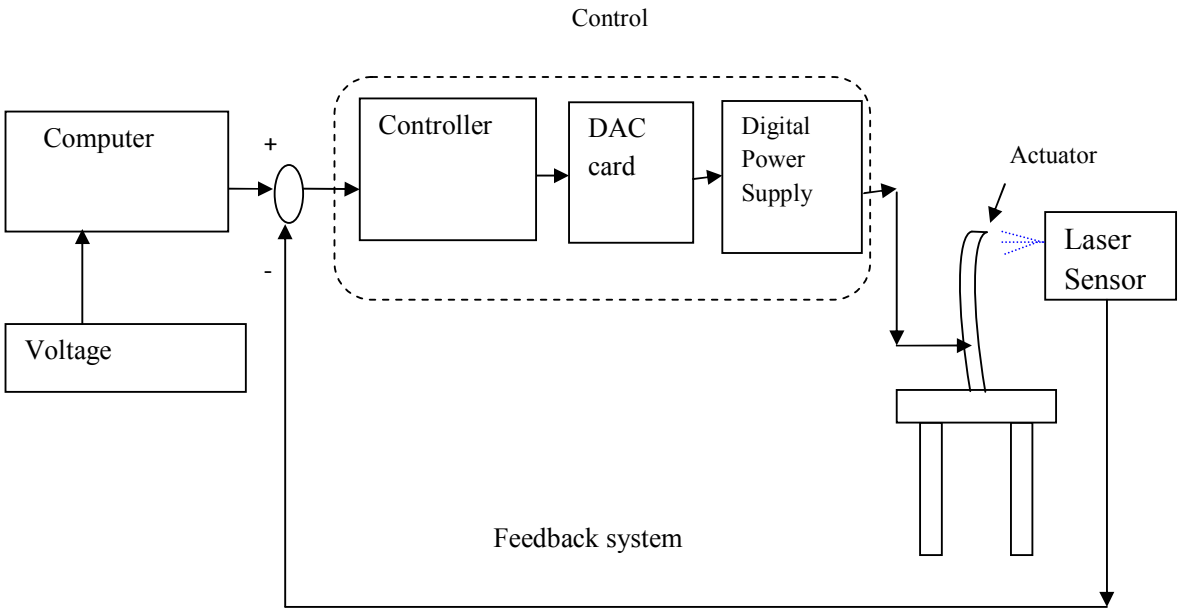

Fig. 11.

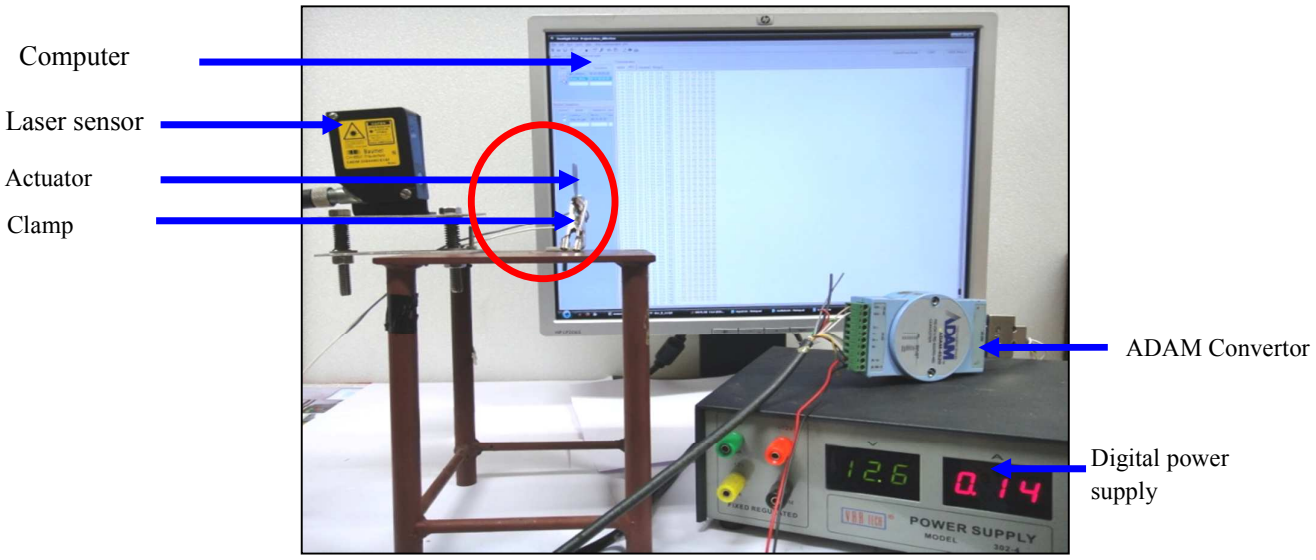

Fig. 12.

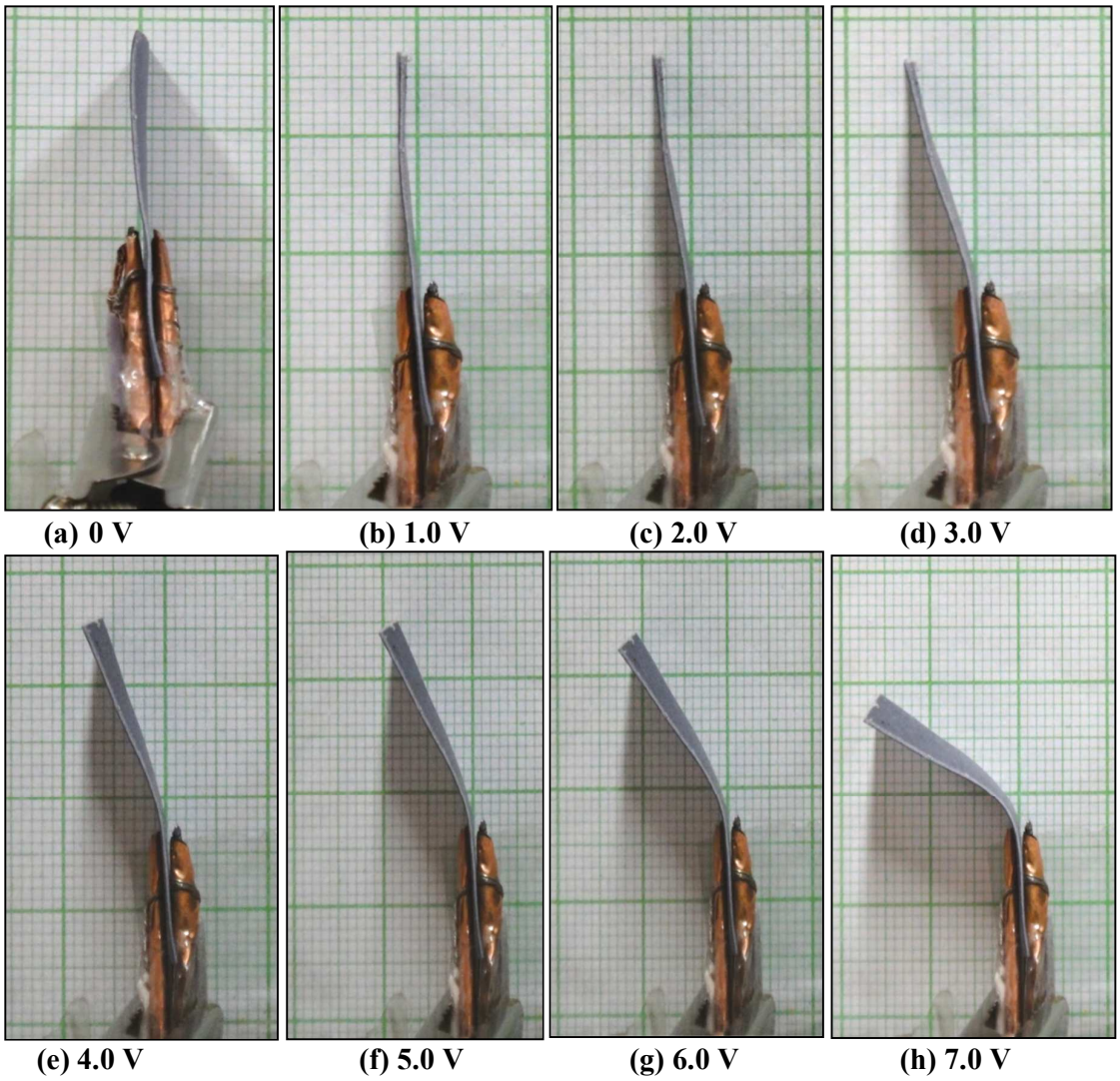

Fig. 13.

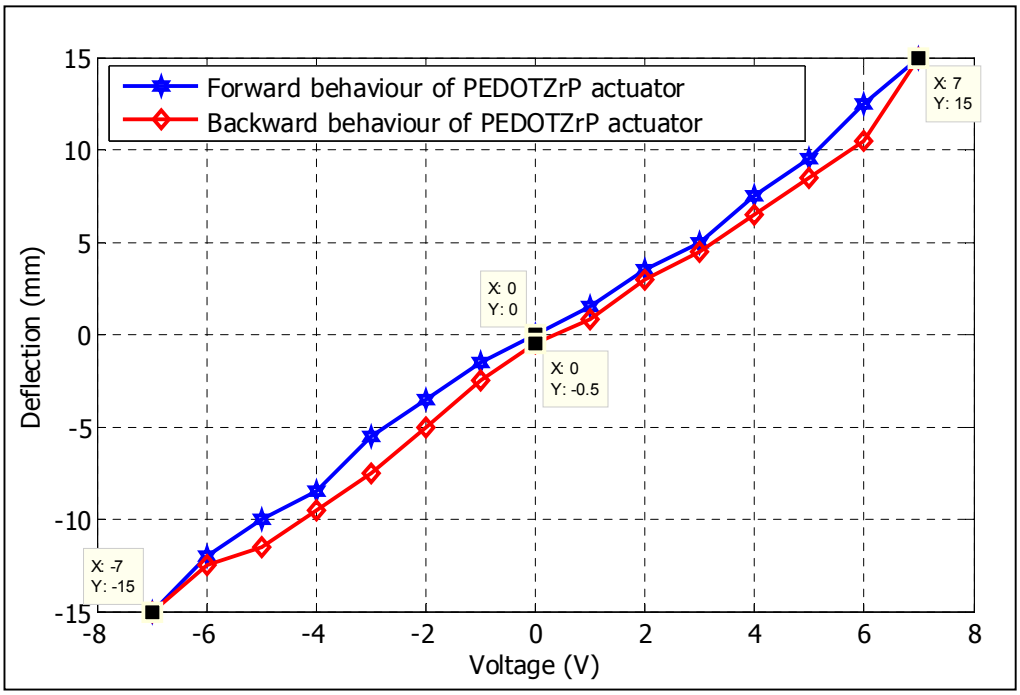

Fig. 14.

Fig. 15.

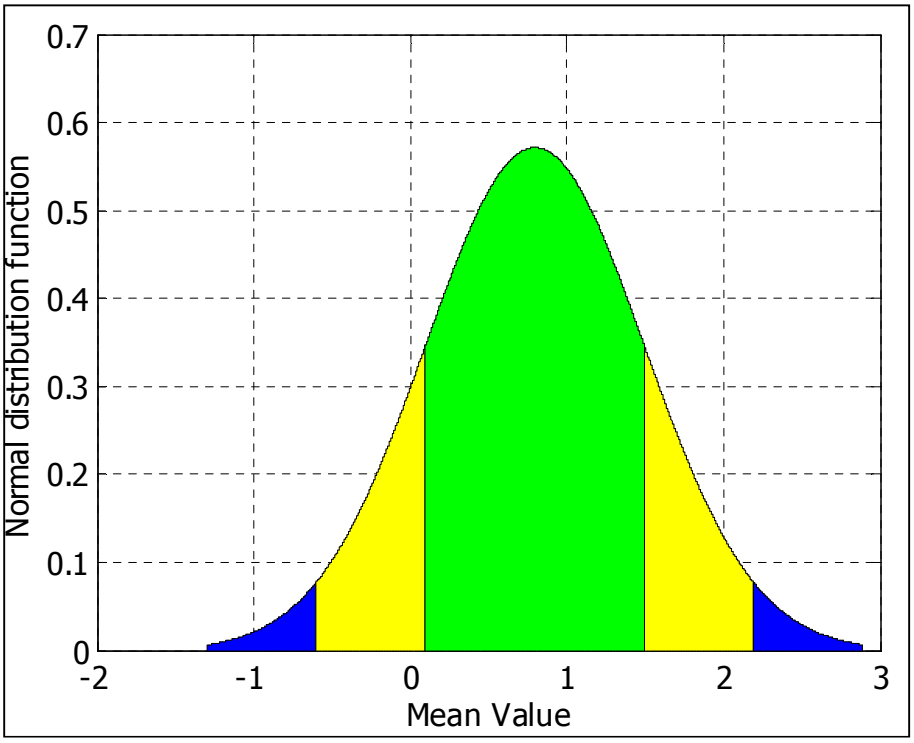

Fig. 16.